



Brazilian Journal of Physics

ISSN: 0103-9733

luizno.bjp@gmail.com

Sociedade Brasileira de Física

Brasil

Shirani, B.; Abbasi, F.

Construction and Experimental Study of a 2.5kJ, Simply Configured, Mather Type Plasma focus device

Brazilian Journal of Physics, vol. 40, núm. 2, junio, 2010, pp. 125-130

Sociedade Brasileira de Física

São Paulo, Brasil

Available in: <http://www.redalyc.org/articulo.oa?id=46415797001>

- How to cite
- Complete issue
- More information about this article
- Journal's homepage in redalyc.org

redalyc.org

Scientific Information System

Network of Scientific Journals from Latin America, the Caribbean, Spain and Portugal

Non-profit academic project, developed under the open access initiative

## Construction and Experimental Study of a 2.5kJ, Simply Configured, Mather Type Plasma focus device

B. Shirani and F. Abbasi\*

Iran, Tehran, Shahid beheshti university, Radiation Application department

(Received on 26 November, 2008)

In this work, a 2.5kJ plasma focus device (named as SBUPF1) has been constructed on the basis of a simple configuration. The most important characteristics of this configuration is relative simplicity and using less components in its structure compared with common configurations. SBUPF1 has been tested between 18-25kV and wide range of pressure for various gases including Argon, Neon and Deuterium. The system shows consistent and reproducible plasma focusing action as well as fusion neutron production (when deuterium is used as working gas).

Keywords: Plasma focus, Pinch, Focusing time, discharge current.

### 1. INTRODUCTION

The plasma focus (PF) devices were developed in the early 1960s Independently by Mather [1] in USA and Filippov [2] in former Soviet Union. The plasma focus is special pulsed power device capable of generating, accelerating and pinching a plasma through the fast electrical discharge of a capacitor bank. The operation of PF has been extensively studied and several PF devices has been developed over the years.

In common configuration of PF [3], the capacitor's H.V electrode connects to anode collector plate through spark gap and connecting cables. Earth electrode of capacitor also connects to cathode collector plate. Discharge current flows in focus tube electrodes through these two plates. Besides, in common configurations for Mather type plasma focus devices, insulator spacers are needed between anode and cathode collector plates [3].

One of the new trends in plasma focus research is using a kind of compact configuration. This configuration has been used in several devices [4-11].

In this configuration, also used in SBUPF1, spark gap directly connects the capacitor to anode, consequently, the anode plate and therefore the spacers are removed.

Focus tube parameters are presented in section 2. In section 3, different devices and the diagnostic equipments employed are described. Section 4 presents the experimental results.

### 2. FOCUS TUBE PARAMETERS

Various device parameters, such as configuration of electrodes and insulator, their dimensions, the materials they are made of, and the initial pressure, are all interrelated in an complicated way. The focusing action and neutron production is possible in wide range of cited parameters. After the primary design, these parameters specially anode length and insulator length can be optimized so as to maximize neutron yield or x-ray intensity [12,13]. For primary design of the focus tube, presented method in [3] has been used. This design is based on a dynamic model [14,15] that considers the focus

dynamics in two separate phases; the axial rundown (shock tube) that crucially delays the radial focus, and pinch phase; until the plasma current has reached its peak value.

Summarizing the design parameters we have:  
 $C_0 = 8.6\mu F$ ,  $L = 190nH$ ,  $V_0 = 24kV$ ,  $a = 1.1cm$ ,  $b = 3.6cm$ ,  $Z_0 = 12cm$ . Where  $L$  is the inductance of the capacitor  $C_0$  together with all connections up to the plasma section of the focus tube,  $V_0$  is the initial charge on the capacitor, 'a' and 'b' are, respectively, the inner and outer radius of the focus tube,  $Z_0$  is length and  $\rho_0$  is the gas density. The insulator that surrounds part of the inner electrode of focus tube has an important role in the plasma focus dynamics. As it is known, soft x-ray and neutron yield strongly depend on the dimensions of the device especially with that of insulator [13]. The neutron yield is relatively low whenever the insulator sleeve length deviates from the optimum value [13]. For plasma focus devices, it is found that a good focusing effect is usually obtained when the insulator sleeve length is in the limited range of  $(b-a) \leq L_{ins} \leq 1.8(b-a)$  [13]. In primary design of SBUPF1, selected length for insulator sleeve is 40mm.

### 3. EXPERIMENTAL ARRANGEMENT

SBUPF1 uses a coaxial capacitor (25kV, 8.6 $\mu F$ ) as energy storage. This capacitor is 41cm in diameter and 74cm in height. Total inductance of discharge circuit is 190nH. an inductance of about 125nH was measured for capacitor by short circuit test. Stored energy in capacitor is discharged through a simple parallel-plate spark gap with a trigatron design (see fig. 1).

The parallel-plate spark gap is made of two 6 cm-diameter brass plates that spaced 13 mm from each other. This space is regulated for discharges between 18–25kV. A thyatron trigger circuit is designed and constructed for triggering the gap. Output pulse of this circuit is applied to trigger electrode and upper plate of spark gap (B and A in fig. 1, respectively) via a 2–m length RG58 cable.

The storage capacitor is charged by a 220V–20kV transformer connected to a HV rectifier diode and a 10k $\Omega$  high power resistor. It takes at least 1min while capacitor reaches to its maximum charge.

The arrangement for the capacitor, spark gap, connected plates and plasma focus tube is shown in fig. 2. Capacitor (fig. 2 no. 1) is placed exactly under the focus tube anode.

\*Electronic address: fabbasi@sbu.ac.ir

Lower plate of spark gap is bolted on central electrode of capacitor via a copper cylindrical connector and upper plate of the spark gap is bolted beneath the 22 cm length, 21mm diameter copper rod. The anode of focus tube is a part of this rod. Earth electrodes of capacitor (16 electrodes) are connected at the edge of cathode plate symmetrically by 16 copper strap, giving a low inductance. The pyrex insulator (fig. 2 no.8) plays an important role in the symmetrical formation of the current sheet and has to be stuck to anode rod. Total length of insulator is 11cm and its thickness is 2mm.

This pyrex thickness can sustain transient voltage differences between anode (no. 16) and cathode plate (no. 14) during plasma focus discharges. The glue should fill the space between anode and pyrex because the glue acts as a vacuum seal.

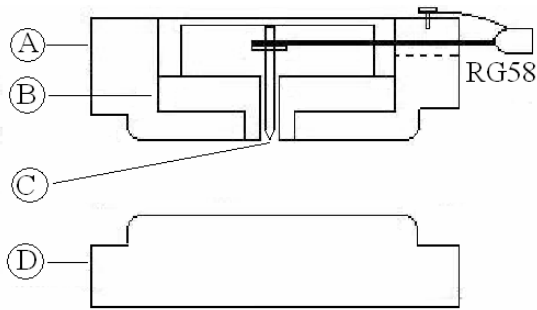


FIG. 1: Parallel-plate spark gap (A and D are brass plates of spark gap, C is trigger electrode and B is insulator).

In addition to sealing the vacuum chamber, O-ring, (fig. 2 no.9) supports the anode rod. Polyethylene disk (fig. 2 no.10) have a 45° groove in which oring rests. This plate is bolted under the cathode plate by three bolts and presses the oring. Anode is regulated vertically relative to cathode plate by these three bolts. The Cathode of focus tube is formed by 12 copper rods, 11cm-length, 1cm diameter, cylindrically placed around the anode.

The plasma chamber (fig. 3) is a 34 cm-height, 18.6 cm-diameter and 3 mm-thickness stainless steel tube. This chamber has four 16.3cm × 4cm plexyglass windows for detecting hard x-rays and for laser diagnostic experiments. Besides, the chamber has four lateral NW25 port for pumping, gas loading, pressure gauging and other purposes.

Vacuum is provided by a single-stage rotary pump reaching an ultimate base pressure about  $4 \times 10^{-3}$  mbar. Pressure is read by a capacitive Gauge connecting to a lateral vacuum port.

After 5 min, because of leakage and outgases from glue, vacuum grease and materials of chamber inner surfaces, pressure is reached to about 0.01 mbar. Operating at a test pressure of 1mbar the impurity in the system is about 1%. This level of vacuum proved to be sufficient for operating with good focus in various gases and good neutron yield when operated in deuterium.

The focus tube electrodes is constructed on the basis of presented values in section 2 and are shown in fig. 4.

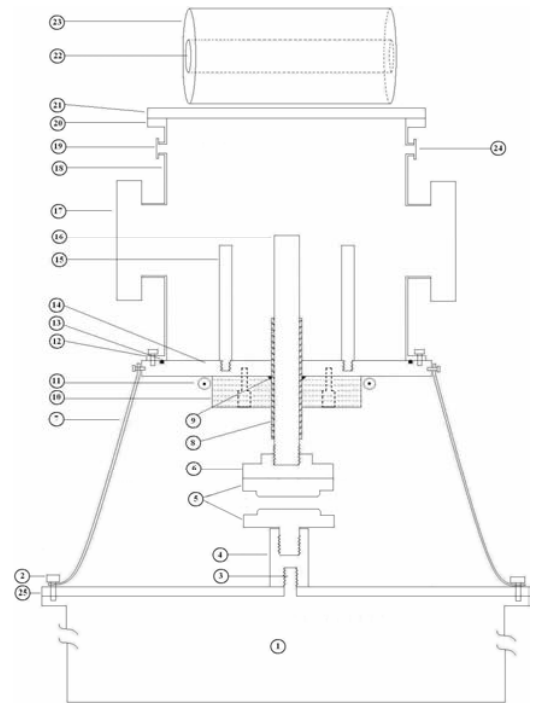


FIG. 2: The arrangement for SBUPF1. 1= 25-kV,8.6- $\mu$ F capacitor; 2 = capacitor Earth stud ; 3 = capacitor H.V electrode ; 4 = connector ; 5 = parallel plate spark gap (indicated with details in fig. 1) ; 6 = connector ; 7 = copper strap ; 8 = pyrex insulator sleeve ; 9 = O-ring seal ; 10 = polyethylene for holding the O-ring ; 11 = Rogowski coil ; 12 = steel flange ; 13 = O-ring seal ; 14 = cathode collector plate ; 15 = focus cathode (12 rods) ; 16 = focus anode ; 17 = chamber window ; 18 = focus chamber ; 19 = outlet to vacuum pump ; 20 = flange ; 21 = back flange ; 22 = the hole for setting detector and foil ; 23 = polyethylene for thermalizing the neutron ; 24 = inlet for test gas ; 25 = insulator cap of capacitor.



FIG. 3: Plasma chamber

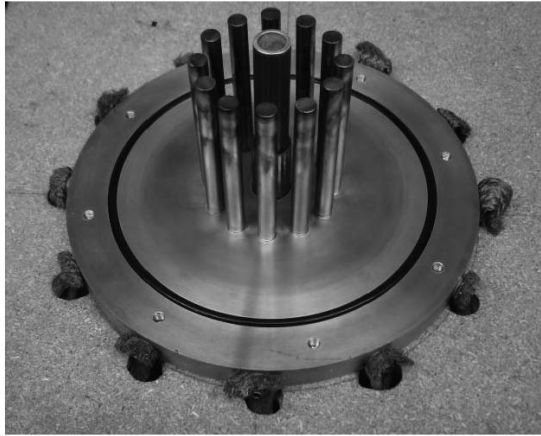


FIG. 4: Focus tube electrodes

To measure the current flowing into the anode, a Rogowski coil (fig. 2 no. 11) and RC integrator circuit with an integration time constant of  $60\mu\text{s}$  displayed on a two channel, 60MHz, 1Gs/s digitizing oscilloscope is used.

Calibration constant for this circuit is about 37 kA/V. For displaying the time derivative of current, Rogowski coil output pulse is directly applied to another channel of oscilloscope by a  $1\Omega$  attenuator.

A silver foil activation system is used to count fusion neutrons from the plasma. This system consists of a 3mm-thick silver foil covering a thin wall Geiger tube. The assembly is placed in center of a 14 cm-diameter polyethylene cylinder so as to thermalize the fusion neutrons.

The detector is placed on the top of plasma chamber perpendicular to the axis of focus tube (fig. 2 no. 22) and is connected to a counter via an inverter, counting fusion neutrons with a calibration constant of  $1.6 \times 10^4$  neutrons per count in first 100-s period after each shot. The counts being taken for two 100-s period immediately after the focus is fired. Calibration is performed with source removal method [16] using a  $^{57}\text{Co}$  Am-Be reference neutron source. In SBUPF1 we also studied the amplitude of neutron signal pulse as detected by a PMT + plastic scintillator.

#### 4. EXPERIMENTAL RESULTS AND CONCLUSION

The system was tested between 18-25kV in various gases including argon, neon and deuterium. A series of about 1200 shots were carried out at different load pressures and the device operation was studied. The relative strength of the plasma focus action is measured by Rogowski coil. In a plasma focus device, the axial drive phase is characterized by a smooth near-sinusoidal rising current. The focus action is indicated in the current dip. Current dip is typical feature of a focus discharge where the large increase of the plasma column impedance has occurred.

In general the stronger the focus, more severely the plasma is compressed and the bigger current dip. The focus system

would be optimized if the input current passing through the electrodes is maximum. This occurs when the focusing is generated i.e. when the current sheet (plasma) formed between the electrodes reaches the top of the inner electrode and is focused. Then it maximizes the magnetic induction and leads to optimum plasma focus. In other words, the plasma axial transit time is equal to the quarter time period of discharge current, and then it becomes the optimized condition for the PFD [17].

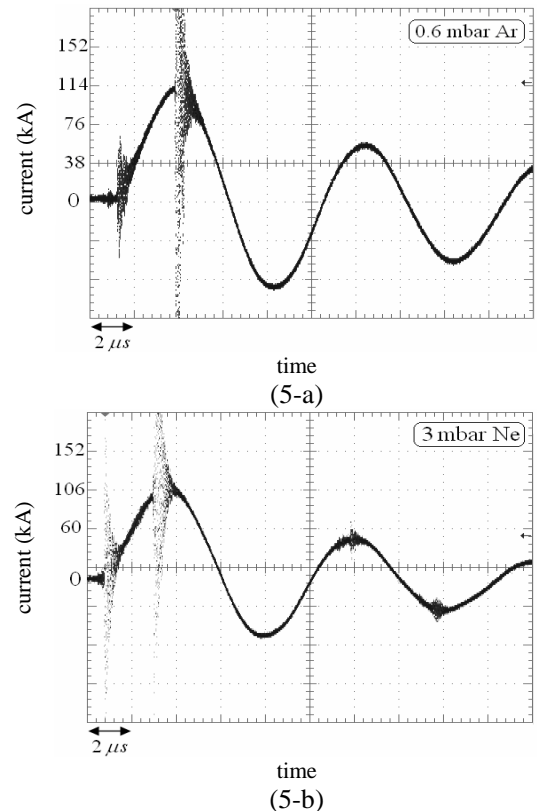


FIG. 5: Typical discharge current signals of SBUPF1 in Argon and Neon.

The system was tested at constant charging voltage 24kV. we obtained the optimum pressure for each gas by changing the filling pressure for optimum focusing condition (i.e. when the current drop occur at the quarter time period.)

Typical current waveforms at 24kV at optimum condition are shown in figure 5 For argon and Neon and in figure 6 for Deuterium. In fig. (6-b) the current derivative of fig. (6-a) has been shown.

From these experiments, it has been found that the characteristic current is about 115kA and the characteristic axial transit time is about  $2.4\mu\text{s}$ . Characteristic current is the amplitude of discharge current and characteristic axial transit time refers to the time that current sheath reaches to anode top.

In argon, at 24kV, the pressure range of focusing is 0.1-1 mbar. It is observed that, as expected, the focus occurs later for higher pressures.

In neon, the pressure range for focusing action is greater

than argon. Focusing action was seen at pressure range of 0.2-5 mbar.

Deuterium shows the greatest range of pressure for focusing. Pressure range of focusing for deuterium is 2-16 mbar.

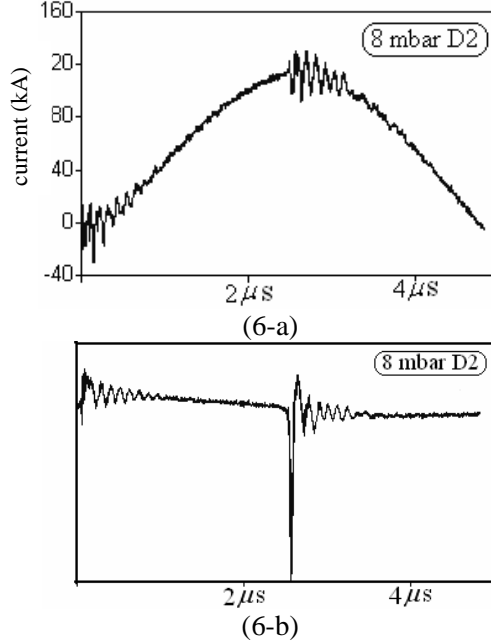


FIG. 6: Typical discharge current signal (a) and current derivative (b) of SBUPF1 in Deuterium.

Table 1 summarizes pressure ranges for optimum focusing, measured in argon, neon and deuterium.

Table 1. Measured optimum pressure ranges for various gases in SBUPF1

Gas	Atomic mass	Optimum pressure range (mbar)
Argon	40	0.3-0.5
Neon	20	1-2.5
Deuterium	2	6-10

These results show little deviation from the snow-plow model prediction.

The characteristic axial transit time, by which the current sheet approaches the top of the inner electrode for the focusing, is explained using the snow-plow model,

$$t_a = \left[ \frac{4\pi^2(c^2 - 1)}{\mu \ln c} \right]^{1/2} \frac{z_0 \rho_0^{1/2}}{(I_0/a)} \quad (1)$$

Where  $t_p, a, b, \mu, z_0, I_0$  and  $\rho_0$  are axial transit time, radius of inner electrode, radius of outer electrode, permeability, length of inner electrode, characteristic current and ambient gas density, respectively and  $c = b/a$  [18].

Gas density is proportional to product of ambient gas pres-

sure and atomic mass according to ideal gas law:

$$\rho = \frac{P \times M}{R \times T} \quad (2)$$

Where  $P, M, R$  and  $T$  are gas pressure, atomic mass of working gas, universal gas constant and temperature, respectively.

Axial transit time is equal to quarter period of discharge current ( $2.4\mu s$  for SBUPF1) at optimum condition.

By replacing the values in equation (1) we have

$$P(\text{mbar}) = \frac{11.77}{M(\text{gr})} \quad (3)$$

Optimum pressure values from table 1 and the prediction by equation 3 are shown in figure 7.

For a gas with higher atomic mass, with the same charging voltage, working pressure should be less to having the same axial transit time and thus to reach the optimum condition.

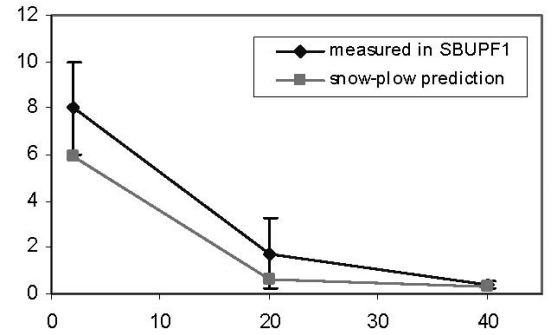


FIG. 7: Variation of optimum pressure (mbar) with atomic mass of working gas

In this work, also we measured the variation of focusing time with discharge voltage at constant pressure for each gas. As expected, the focus occurs later for lower discharge voltages. Figure 8 shows the average dependence of the focusing time with the primary voltage of capacitor.

The system was tested in deuterium with 2.5kJ stored energy at pressure range of 1-18 mbar.

Optimum pressure for maximum neutron yield is 8mbar and in this pressure, counts of 800-3000 are obtained at a 100-s period after shot. This corresponds to about  $2 - 8 \times 10^7$  neutrons per shot. Figure 9 shows the variation of the neutron yield with deuterium filling pressure.

A typical oscillogram of neutron pulse is given in figure 10. neutron pulse is generated by plastic scintillator detector mounted at a distance of 4m from anode top.

4 main peaks are seen in this pulse. This is the evidence that neutron is produced at two separate phases. Time interval between these two phases is about 45ns.

Two first peaks are generated by hard x-ray photons and next two peaks are produced by neutrons. Neutrons have entered to detector with a delay of about 180ns after photons. This flight time is equivalent to an average energy of about 2.24MeV for neutrons.

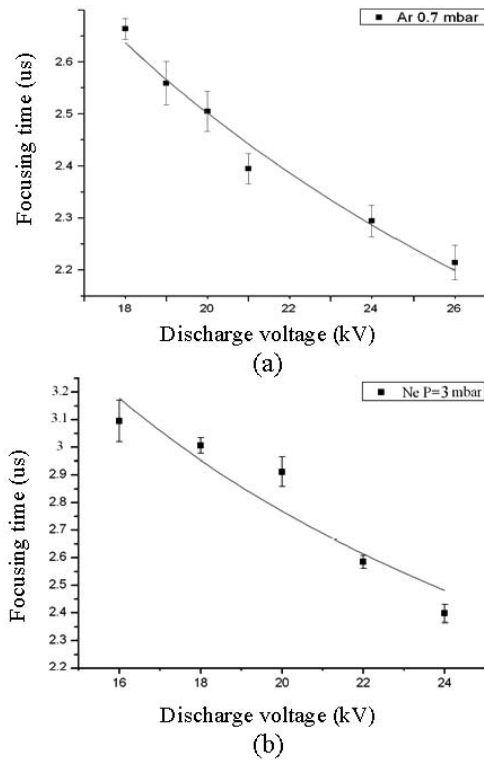


FIG. 8: Variation of focusing time with discharge voltage in argon and neon

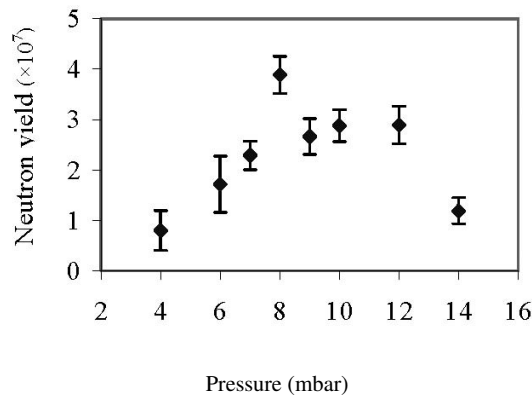


FIG. 9: Neutron yield vs. Deuterium filling pressure at 2.5kJ working energy

Although only a fraction of the initial energy stored,  $E$ , in the capacitor bank is transferred to the plasma, the parameter  $E/V_p \sim 28E/a^3$  (with the plasma volume  $V_p$ ) is usually used to characterize the plasma energy density in order to compare different devices [8]. The energy density parameter is of the order of  $(1-10) \times 10^{10} Jm^{-3}$  for a wide range of PF energies. [8]

Another relevant parameter in plasma focus is the drive

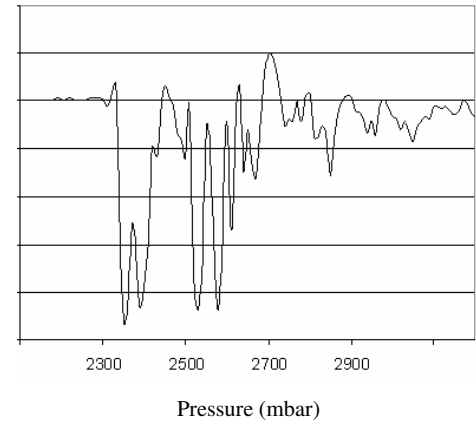


FIG. 10: A typical neutron pulse in SBUPF1

parameter  $(I_0/ap^{1/2})$ , where  $I_0$  is the peak current,  $a$  is the anode radius and  $p$  is the gas filling pressure for the maximum neutron yield. This drive parameter  $(I_0/ap^{1/2})$  is related to the velocity of the axial and radial phases of the plasma motion (of the order of  $v_a = (0.8 - 1) \times 10^5$  and  $v_r = (2 - 2.5) \times 10^5 m s^{-1}$ , respectively, for a wide range of PF sizes). In fact, the axial and radial velocities are proportional to  $(I_0/ap^{1/2})$ . For devices in the range of 3 kJ – 1 MJ operating in deuterium, the drive parameter is  $(I_0/ap^{1/2}) = 77 \pm 7 kAcm^{-1} mbar^{1/2}$ . [8]

Even though the energy density parameter is in the order of magnitude for SBUPF1 device,  $5 \times 10^{10} Jm^{-3}$ , the drive parameter gives a value of  $37 kA/cm.mbar^{1/2}$ , this value is half of the recommended value. This is probably due to the low current limited by the high inductance of the device.

In order to optimize the device, it could be useful to produce a coaxial geometry for copper traps (fig. 2 No. 7) and spark gap and decrease length of them to decreasing total inductance. One way is replacing the traps by a copper cylinder to connects the cathode plate to cathode of capacitor.

One of the future works to increase neutron yield of SBUPF1 is determining optimum length of the insulator. Length of 4mm has been chosen from limited range of reference [13]. The insulator length should be changed between 2.5mm & 4.5mm, thus the optimum length will be found. These optimizations, certainly will result to higher neutron yield.

In structure of SBUPF1, less number of components and less connections are used compared with conventional configuration of PF devices. Moreover, neutron yield of SBUPF1 is almost equal to yield of other devices working at same range of energy. Zakaullah et. al. [12] have reported  $1.3 \times 10^8$  neutrons/shot for a 2.3kJ device at optimum anode length and optimum pressure.

Shyam and Rout [19] have reported  $10^8$  n/shot for a 2.2kJ plasma focus at optimum conditions.

SBUPF1 is not a portable device, But, according to its good focusing action, neutron production and simplification in structure, this configuration could be a better choice for compact and portable PF neutron sources that will be designed to be used in field applications such as well logging

and land mine detection.. SBUPF1 is designed and constructed to be used at research in the field of radiation appli-

cations such as non-destructive testing and material inspection.

- 
- [1] J.W. Mather, Phys. Fluids, vol. **8**(2), 366 (1965).
  - [2] Filippov N. Filipova T. and Vinogradov V. : N. Fusion Suppl. Pt. **2**, 577 (1962).
  - [3] Lee et. al. Am. J. Phys. **56**(1) (1988).
  - [4] L. Soto et al, Physics of Plasma **8**, 2572 (2001).
  - [5] P. Silva et al, Rev. Sci. Instrum. **73**, 2583 (2002).
  - [6] P. Silva et al. App. Phys. Lett. **83**, 3269 (2003).
  - [7] P. Silva et al. Plasma Sources: Sci. And Technol. **13**, 329 (2004).
  - [8] L. Soto, Plasma Physics and Controlled Fusion **47**, A361 (2005).
  - [9] L. Soto et al, J. Phys. D: App. Phys. **41**, 205215 (2008).
  - [10] R. K. Rout et al, J. Phys. D: Appl. Phys. **41**, 205211 (2008).
  - [11] R. Verma et al, Plasma Sources Sci. Technol. **17**, 045020 (2008).
  - [12] M. Zakaullah , G. Murtaza, I. Ahmad, F. N. Beg, M. M. Beg and M. shabbir Plasma Sources Sci. and Technol. **4** 117-124 (1995).
  - [13] H. R. Yousefi et al., Physics Letters **A 361** 360-363 (2007).
  - [14] S. Lee, in Laser and Plasma Technology, edited by S. Lee, B. C. Tan, C. S. Wong, and A. C. Chew (World Scientific, Singapore, 1985), pp. 37, 64, and 387.
  - [15] S. Lee, in Radiation in Plasma, edited by B. Namara (World Scientific, Singapore, 1984), Vol. 11, p. 978.
  - [16] A. Gentilini et al Nucl. Instr. and Meth. **172**, 541-552 (1980).
  - [17] H. J. Woo, et. al. Plasma Phys. Control. Fusion **46**, 1095-1104 (2004).
  - [18] S. Lee and A. Serban, IEEE trans. on plasma sci. **24**, 1101 (1996).
  - [19] R. K. Rout et. al., IEEE trans. on Plasma Sci. **23**, 996 (1995).